

Quantum teleportation between particlelike and fieldlike qubits using hybrid entanglement under decoherence effects

Kimin Park, Seung-Woo Lee, and Hyunseok Jeong*

Center for Macroscopic Quantum Control, Department of Physics and Astronomy, Seoul National University, Seoul 151-742, Korea

(Received 14 September 2012; published 3 December 2012)

We study quantum teleportation between two different types of optical qubits, one of which is “particlelike” and the other “fieldlike,” via hybrid entangled states under the effects of decoherence. We find that teleportation from particlelike to fieldlike qubits can be achieved with a higher fidelity than that in the opposite direction. However, teleportation from fieldlike to particlelike qubits is found to be more efficient in terms of the success probabilities. Our study shows that the direction of teleportation should be considered an important factor in developing optical hybrid architectures for quantum information processing.

DOI: [10.1103/PhysRevA.86.062301](https://doi.org/10.1103/PhysRevA.86.062301)

PACS number(s): 03.67.Hk, 42.50.Ex, 03.65.Yz

I. INTRODUCTION

In optical implementations of quantum information processing (QIP), some physical degrees of freedom of light are used for qubit encoding [1–3]. For example, horizontal and vertical polarization states $|H\rangle$ and $|V\rangle$ of a single photon may be used to form a qubit basis. This type of encoding is referred to as *particlelike* encoding [3] because individual photons are information carriers. It is also called dual-rail encoding as it uses two distinct optical modes for a qubit [4]. In this type of approach, single-qubit gates can be easily realized using linear optics elements, while two-qubit operations are generally difficult to implement. Alternatively, one may encode information into two distinct states of a field mode such as the vacuum and single-photon [5] or two coherent states of distinct amplitudes [6–9]. This type of encoding is called *fieldlike* encoding (or single-rail encoding) [3]. The coherent-state encoding has advantages for the Bell-state measurement [10,11], and quantum computation schemes [7,8] based on its distinctive teleportation method [10,12] have been developed. Each of the two encoding schemes has its own advantages and disadvantages for QIP [13,14].

There have been studies on QIP based on hybrid structures using both particlelike and fieldlike features of light [15–21]. This type of “hybrid architecture” may be used to make up for the weaknesses in both types of qubit structures. Indeed, a near-deterministic universal quantum computation with a relatively small number of resources is found to be possible using linear optics with a hybrid qubit composed of photon polarization and a coherent state [21]. In this regard, it is important to fully investigate such hybrid architectures, and information transfer between different types of qubits would be a crucial task. The quantum teleportation protocol [22,23] can be used for such information transfer from one type of system to another. For example, Ralph *et al.* discussed a scheme to perform teleportation between dual-rail (polarization) and single-rail (vacuum and single-photon) qubits [24]. In addition, in order to address practical conditions for such information transfer, it would also be important to include decoherence effects caused by photon losses that are typical in optical systems.

In this paper, we study quantum teleportation between particlelike and fieldlike qubits under decoherence effects. We first consider teleportation between polarization and coherent-state qubits and that between a polarization qubit and a qubit of the vacuum and single photon. In our study, in general, teleportation from particlelike to fieldlike qubits shows higher fidelities under decoherence effects compared to teleportation in the opposite direction. However, teleportation from fieldlike to particlelike qubits is, in general, more efficient in terms of the success probabilities. This implies that the “direction” of teleportation should be considered to be an important factor when developing optical hybrid architectures for QIP.

This paper is organized as follows: In Sec. II, the time evolution of the two hybrid entangled states under photon losses is investigated. The degrees of entanglement for the hybrid channels are calculated in Sec. III. The average fidelities and success probabilities of teleportation are in Secs. IV and V. Section IV deals with teleportation between polarization and coherent-state qubits while Sec. V is devoted to investigate teleportation between polarization and single-rail Fock state qubits. In Sec. VI, the issue of postselection is discussed and investigated. We conclude the paper with final remarks in Sec. VII.

II. TIME EVOLUTION OF TELEPORTATION CHANNELS

The first kind of teleportation channel considered in this paper is a hybrid entangled state of the photon polarization and coherent state:

$$|\psi_{pc}\rangle = \frac{1}{\sqrt{2}}(|H\rangle_p|\alpha\rangle_c + |V\rangle_p|-\alpha\rangle_c), \quad (1)$$

where $|\pm\alpha\rangle$ are coherent states of amplitudes $\pm\alpha$. We assume that α is real for simplicity throughout the paper without loss of generality. The other one is a hybrid channel of the photon polarization and the single-rail photonic qubit:

$$|\psi_{ps}\rangle = \frac{1}{\sqrt{2}}(|H\rangle_p|0\rangle_s + |V\rangle_p|1\rangle_s), \quad (2)$$

where $|0\rangle$ and $|1\rangle$ denote the vacuum and the single photon state in the Fock basis, respectively, comprising a fieldlike (single-rail) qubit. Here, p, c, and s respectively stand for polarization, coherent-state, and single-rail Fock-state qubits. It is known that the hybrid channel $|\psi_{pc}\rangle$ can in principle

*h.jeong37@gmail.com

be produced using a weak cross-Kerr nonlinear interaction between a polarization (dual-rail) single-photon qubit and a coherent state [15,17,25]. However, it is highly challenging to perform the required nonlinear interaction with high efficiency [26–28]. The hybrid channel $|\psi_{ps}\rangle$ can be generated using a parametric down conversion, a Bell state measurement with polarization qubits, and an adaptive measurement [24].

We consider decoherence caused by photon loss (dissipation) on the teleportation channels. The dissipation for state ρ is described by the master equation under the Born-Markov approximation with a zero-temperature environment [29]:

$$\frac{\partial \rho}{\partial \tau} = \hat{J}\rho + \hat{L}\rho, \quad (3)$$

where τ is the system-bath interaction time. Lindblad superoperators \hat{J} and \hat{L} are defined as $\hat{J}\rho = \gamma \sum_i a_i \rho a_i^\dagger$ and $\hat{L}\rho = -\sum_i \gamma (a_i^\dagger a_i \rho + \rho a_i^\dagger a_i)/2$, where γ is the decay constant determined by the coupling strength of the system and environment, and a_i is the annihilation operator for mode i . Throughout this paper, we assume that the decay constant γ is the same for modes p , c , and s (i.e., the photon loss occurs at the same rate for all modes).

The formal solution of Eq. (3) is written as $\rho(\tau) = \exp[(\hat{J} + \hat{L})\tau]\rho(0)$, where $\rho(0)$ is the initial density operator at $\tau = 0$. By solving this equation we obtain the decohered density matrix for the initial state of the hybrid channel $|\psi_{pc}\rangle$ in Eq. (1) as

$$\begin{aligned} \rho_{pc}(t; \alpha) = & \frac{1}{2}[\{t^2|H\rangle_p\langle H| + (1-t^2)|0\rangle_p\langle 0|\} \otimes |t\alpha\rangle_c\langle t\alpha| \\ & + \{t^2|V\rangle_p\langle V| + (1-t^2)|0\rangle_p\langle 0|\} \otimes |-t\alpha\rangle_c\langle -t\alpha| \\ & + t^2 Q(t)(|H\rangle_p\langle V| \otimes |t\alpha\rangle_c\langle -t\alpha| + \text{H.c.})], \end{aligned} \quad (4)$$

where the parameter $t = e^{-\gamma\tau/2}$ describes the amplitude decay, and $Q(t) \equiv \exp[-2\alpha^2(1-t^2)]$ reflects the reduction of the off-diagonal coherent-state dyadic $|\alpha\rangle\langle -\alpha|$ and its Hermitian conjugate. We define the normalized time as $r = (1-t^2)^{1/2}$ which gives a value $r = 0$ at $\tau = 0$ and $r = 1$ at $\tau = \infty$. Likewise, we obtain the decohered density matrix $\rho_{ps}(t)$ for the initial state in the channel in Eq. (2) as

$$\begin{aligned} \rho_{ps}(t) = & \frac{1}{2}[\{t^2|H\rangle_p\langle H| + (1-t^2)|0\rangle_p\langle 0|\} \otimes |0\rangle_s\langle 0| \\ & + \{t^2|V\rangle_p\langle V| + (1-t^2)|0\rangle_p\langle 0|\} \otimes \{t^2|1\rangle_s\langle 1| \\ & + (1-t^2)|0\rangle_s\langle 0|\} + t^3(|H\rangle_p\langle V| \otimes |0\rangle_s\langle 1| + \text{H.c.})]. \end{aligned} \quad (5)$$

As shown in Eqs. (4) and (5), photon loss induces (i) the decay of the amplitude of coherent state as $|\alpha\rangle \rightarrow |t\alpha\rangle$, (ii) the transition of polarization states $|H\rangle_p\langle H|$ and $|V\rangle_p\langle V|$ into the vacuum state $|0\rangle_p\langle 0|$, which causes an escape error out of the qubit space, (iii) the transition of the single-photon Fock state $|1\rangle_s\langle 1|$ into the vacuum state $|0\rangle_s\langle 0|$, which is a flip error of the qubit, and (iv) the decrease of the coefficients of coherence (off-diagonal) terms with $t^2 Q(t)$ in Eq. (4) and t^3 in Eq. (5).

III. ENTANGLEMENT OF HYBRID CHANNELS

The negativity of state ρ , known as a measure of entanglement, is defined as [30,31]

$$N(\rho) = \|\rho^{T_B}\| - 1 = 2 \sum_{\lambda_i < 0} |\lambda_i|, \quad (6)$$

where ρ^{T_B} is the partial transpose of ρ about one mode of composite system (say mode B here), $\|\cdot\|$ denotes the trace norm and the λ_i are negative eigenvalues of ρ^{T_B} . We calculate the negativity of the decohered channel ρ_{pc} given in Eq. (4) as

$$\begin{aligned} N(\rho_{pc}(t; \alpha)) & = \frac{t^2}{2N_+^2 N_-^2} \left\{ [Q(t) - 1](N_+^2 + N_-^2) \right. \\ & \left. + \sqrt{16Q(t)N_+^2 N_-^2 + [1 - Q(t)]^2(N_+^2 + N_-^2)^2} \right\}, \end{aligned} \quad (7)$$

where $N_\pm = [2 \pm 2 \exp(-2t^2\alpha^2)]^{-1/2}$ are normalization factors for equal superpositions of coherent states $|\pm\rangle = N_\pm(|t\alpha\rangle \pm |-t\alpha\rangle)$. This is obtained by representing the coherent-state-qubit part of Eq. (4) in the orthogonal basis $\{|\pm\rangle\}$ and performing calculations following Eq. (6). The negativity of the decohered entangled channel ρ_{ps} in Eq. (5) is also obtained as

$$N(\rho_{ps}) = t^4. \quad (8)$$

The degrees of entanglement for the two channels are plotted in Fig. 1, and we find that entanglement contained in $|\psi_{ps}\rangle$ is more robust to decoherence than that of $|\psi_{pc}\rangle$. Obviously, state $|\psi_{pc}\rangle$ is more entangled when α is larger at the initial time. As $\alpha \rightarrow 0$, the initial state approaches a product state with no entanglement. However, when the initial value of α is larger, the slope of the decrease of entanglement is steeper (i.e., entanglement disappears more rapidly). The reason for this is that state $|\psi_{pc}\rangle$ becomes a more ‘‘macroscopic’’ quantum superposition, fragile to decoherence, when α is large. This feature has been pointed out in a number of previous studies [10,32–35] with various versions of continuous-variable superpositions and entangled states. In our case, when $\alpha \approx 1$,

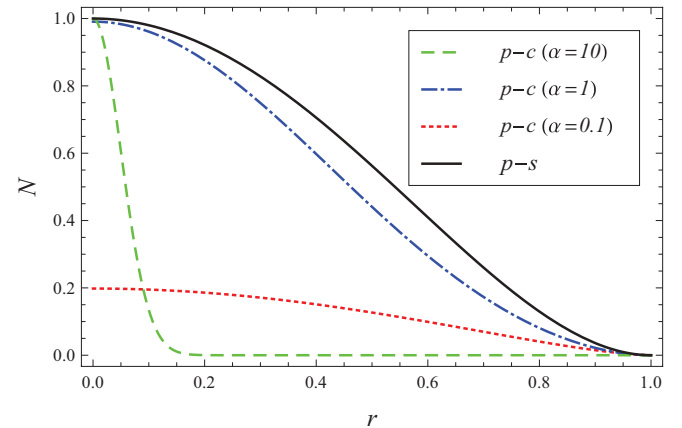


FIG. 1. (Color online) Negativity N of hybrid channels ρ_{pc} (dotted, dot-dashed, and dashed curves) and ρ_{ps} (solid curve) in Eqs. (4) and (5), against the normalized time r under decoherence.

entanglement seems most robust to decoherence considering both the initial value and the decreased slope of entanglement.

IV. TELEPORTATION BETWEEN POLARIZATION AND COHERENT-STATE QUBITS

We now consider quantum teleportation using the hybrid channels. Besides the hybrid channels, Bell-state measurements and single-qubit unitary transforms, σ_x and σ_z operations, at the receiver's site are required to complete the teleportation process. In order to avoid unrealistic assumptions, we assume throughout the paper that only linear optics elements are available besides the hybrid quantum channels.

In this section, we first investigate quantum teleportation between polarization and coherent-state qubits through the decohered entangled state ρ_{pc} in Eq. (4). For convenience, we use the arrow $A \rightarrow B$ for the teleportation from qubit type A to type B when a hybrid entangled state composed of two qubits with types A and B is used as the teleportation channel. For example, $p \rightarrow c$ indicates teleportation from polarization to coherent-state qubits, and vice versa for $c \rightarrow p$.

A. Teleportation fidelities

The teleportation fidelity F is defined as $F = \langle \psi_t | \rho_{out} | \psi_t \rangle$ where $|\psi_t\rangle$ is the target state of teleportation and ρ_{out} is the density operator of the output qubit. Due to the nonorthogonality of two coherent states, it is not trivial to define the fidelity between a polarization qubit and a coherent-state qubit. In the case of teleportation from a polarization qubit, $|\psi_t\rangle_p = a |H\rangle_p + b |V\rangle_p$, to a coherent-state qubit, it would be reasonable to choose the target state as

$$|\psi_t\rangle_c = N(a |t\alpha\rangle_c + b |-t\alpha\rangle_c), \tag{9}$$

where $N = \{1 + (ab^* + a^*b) \exp(-2t^2\alpha^2)\}^{-1/2}$ is the normalization factor. We note that we take a dynamic qubit basis $\{|\pm t\alpha\rangle\}$ in order to reflect the decrease of the amplitude under photon losses [10], and that t is considered a known value. Conversely, for the teleportation of opposite direction ($c \rightarrow p$) the state in Eq. (9) is considered the input qubit and $|\psi_t\rangle_p = a |H\rangle_p + b |V\rangle_p$ is considered the target state.

The Bell-state measurement, an essential part of quantum teleportation, discriminates four Bell states:

$$|B_{1,2}\rangle_{pp'} = \frac{1}{\sqrt{2}}(|H\rangle_p |H\rangle_{p'} \pm |V\rangle_p |V\rangle_{p'}), \tag{10}$$

$$|B_{3,4}\rangle_{pp'} = \frac{1}{\sqrt{2}}(|H\rangle_p |V\rangle_{p'} \pm |V\rangle_p |H\rangle_{p'}). \tag{11}$$

The Bell-state measurement in polarization modes can be performed by a 50 : 50 beam splitter, two polarizing beam splitters, and photon detectors [36], which discriminates only $|B_{3,4}\rangle_{pp'}$ successfully. The net effect of this process is equivalent to taking the inner product of the total density matrix $|\psi_t\rangle_p \langle \psi_t| \otimes \rho_{p'c}(t; \alpha)$ with a Bell state, and an appropriate unitary transform is applied to reconstruct the original state. For example, when one of the Bell states, $|B_1\rangle_{pp'}$, is measured, the output state for the teleportation from a polarization to a coherent-state qubit for an input state $|\psi_t\rangle_p$ is given as

$$\rho_{out}^{p \rightarrow c} = \frac{{}_{pp'}\langle B_1 | \{ |\psi_t\rangle_p \langle \psi_t| \otimes \rho_{p'c}(t; \alpha) \} | B_1 \rangle_{pp'}}{\text{Tr}[|B_1\rangle_{pp'} \langle B_1| \{ |\psi_t\rangle_p \langle \psi_t| \otimes \rho_{p'c}(t; \alpha) \}]} \tag{12}$$

In this case, no unitary transform is required. In the cases of the other outcomes, the required unitary transforms for the coherent-state part are

$$\begin{aligned} Z_c &: |\pm t\alpha\rangle_c \rightarrow \pm |\pm t\alpha\rangle_c, \\ X_c &: |\pm t\alpha\rangle_c \rightarrow |\mp t\alpha\rangle_c, \end{aligned} \tag{13}$$

after which the state of Eq. (12) is obtained. One or both of these operations should be applied depending on the Bell-state measurement outcome [10]. It is relatively easy to perform X_c using phase shifter, while the implementation of Z_c is nontrivial [10,13]. The displacement operation can approximate the Z_c operation [7,10] but it becomes effective only for $\alpha \gg 1$.

Therefore, we slightly modify the Bell measurement to obtain different success outcomes (instead of $|B_{3,4}\rangle_{pp'}$) to avoid the Z_c operation. A Hadamard operation on the first mode, and a bit-flip operator X with a Hadamard operation on the second input mode in $\{|H\rangle, |V\rangle\}$ basis respectively transforms the Bell states to

$$|B_1\rangle_{pp'} \rightarrow |B_3\rangle_{pp'}, \quad |B_2\rangle_{pp'} \rightarrow |B_1\rangle_{pp'}, \tag{14}$$

$$|B_3\rangle_{pp'} \rightarrow |B_4\rangle_{pp'}, \quad |B_4\rangle_{pp'} \rightarrow |B_2\rangle_{pp'}. \tag{15}$$

When the Bell-measurement setup is applied after this transformation, we can discriminate the initial states $|B_1\rangle_{pp'}$ and $|B_3\rangle_{pp'}$ before the above transformation as successful outcomes. In this way, only the X_c operation is necessary on the output state of teleportation.

Inserting explicit forms of $\rho_{p'c}(t; \alpha)$ in Eq. (4) and $|\psi_t\rangle_p = a |H\rangle_p + b |V\rangle_p$ into (12) gives

$$\rho_{out}^{p \rightarrow c} = \frac{|a|^2 |t\alpha\rangle_c \langle t\alpha| + |b|^2 |-t\alpha\rangle_c \langle -t\alpha| + Q(t)(ab^* |t\alpha\rangle_c \langle -t\alpha| + a^*b |-t\alpha\rangle_c \langle t\alpha|)}{1 + e^{-2\alpha^2}(ab^* + a^*b)}. \tag{16}$$

We find the fidelity between the output state $\rho_{out}^{p \rightarrow c}$ in Eq. (16) and the target state $|\psi_t\rangle_c = N(a |t\alpha\rangle_c + b |-t\alpha\rangle_c)$ as

$$F_{p \rightarrow c} = \langle \psi_t | \rho_{out}^{p \rightarrow c} | \psi_t \rangle_c = \frac{|a|^2 |a + bS|^2 + |b|^2 |aS + b|^2 + 2Q(t)\text{Re}[ab^*(a + bS)(a^*S + b^*)]}{N^{-2}\{1 + e^{-2\alpha^2}(ab^* + a^*b)\}}, \tag{17}$$

where $S = \langle t\alpha | -t\alpha \rangle = \exp(-2t^2\alpha^2)$ is the overlap between the dynamic qubit basis states.

We now find the average teleportation fidelity over all possible input states. For convenience, we parametrize the unknown values of the input state as $a = \cos[\theta/2] \exp[i\phi/2]$ and $b = \sin[\theta/2] \exp[-i\phi/2]$, where $0 \leq \phi < 2\pi$ and $0 \leq \theta < \pi$. The

average of $F_{p \rightarrow c}(\theta, \phi)$ in Eq. (17) over all input states is then obtained using Eq. (19) as

$$F_{p \rightarrow c}(t) = \langle F_{p \rightarrow c}(\theta, \phi) \rangle_{\theta, \phi} = \frac{1}{4\pi} \int_0^\pi d\theta \sin \theta \int_0^{2\pi} d\phi F_{p \rightarrow c}(\theta, \phi) \\ = \frac{Q(t)}{Q(t) - 1} \{2G[|a|^4] + [2S^2 + 2Q(t)]G[|a|^2|b|^2] + [SQ(t) + S]G[ab^* + a^*b] + S^2Q(t)G[a^2b^{*2} + a^{*2}b^2]\}, \quad (18)$$

where $G[f]$ for arbitrary value or function $f = f(\theta, \phi)$ is

$$G[f] = \left\langle \frac{f}{1 + Q(t)S(ab^* + a^*b)} - \frac{f}{1 + S(ab^* + a^*b)} \right\rangle_{\theta, \phi}, \quad (19)$$

with

$$\left\langle \frac{|a|^4}{1 + x(ab^* + a^*b)} \right\rangle_{\theta, \phi} = \frac{x + \frac{-1+3x^3}{\tanh[x]}}{8x^3}, \quad (20)$$

$$\left\langle \frac{|a|^2|b|^2}{1 + x(ab^* + a^*b)} \right\rangle_{\theta, \phi} = -\frac{x + \frac{-1-x^2}{\tanh[x]}}{8x^3}, \quad (21)$$

$$\left\langle \frac{ab^* + a^*b}{1 + x(ab^* + a^*b)} \right\rangle_{\theta, \phi} = \frac{1}{x} - \ln \left[\frac{1+x}{1-x} \right] \frac{1}{2x^2}, \quad (22)$$

$$\left\langle \frac{a^2b^{*2} + a^{*2}b^2}{1 + x(ab^* + a^*b)} \right\rangle_{\theta, \phi} = \frac{2-x^2}{4x^3} \ln \left[\frac{1+x}{1-x} \right] - \frac{1}{x^2}, \quad (23)$$

for arbitrary value x independent of θ and ϕ .

Now, we consider teleportation from a coherent-state qubit to a polarization qubit. The Bell-state measurement for coherent-state qubits can be performed using a 50:50 beam splitter and two photon-number parity measurements [10]. The input qubit of the form of Eq. (9) together with the coherent-state part of channel $\rho_{pc}(t; \alpha)$ passes through the 50:50 beam splitter and evolves as

$$(a|\beta\rangle + b|-\beta\rangle)_{c|\beta\rangle_{c'}} \rightarrow a|\sqrt{2}\beta\rangle_{c|0\rangle_{c'}} + b|0\rangle_{c|\sqrt{2}\beta\rangle_{c'}} \\ (a|\beta\rangle + b|-\beta\rangle)_{c|-\beta\rangle_{c'}} \rightarrow a|0\rangle_{c|-\sqrt{2}\beta\rangle_{c'}} \\ + b|-\sqrt{2}\beta\rangle_{c|0\rangle_{c'}}, \quad (24)$$

where $\beta = t\alpha$. We note that the photons move to either of the two modes so that only one of the two detectors can detect any photon(s). The projection operators O_j for the outcomes j of the two parity measurements can then be written as

$$\hat{O}_1 = \sum_{n=1}^{\infty} |2n\rangle_A \langle 2n| \otimes |0\rangle_B \langle 0|, \quad (25)$$

$$\hat{O}_2 = \sum_{n=1}^{\infty} |2n-1\rangle_A \langle 2n-1| \otimes |0\rangle_B \langle 0|, \quad (26)$$

$$\hat{O}_3 = \sum_{n=1}^{\infty} |0\rangle_A \langle 0| \otimes |2n\rangle_B \langle 2n|, \quad (27)$$

$$\hat{O}_4 = \sum_{n=1}^{\infty} |0\rangle_A \langle 0| \otimes |2n-1\rangle_B \langle 2n-1|, \quad (28)$$

where subscripts 1, 2, 3, and 4 represent the four Bell states

$$|\mathcal{B}_{1,2}\rangle_{cc'} \propto |\alpha\rangle_c |\alpha\rangle_{c'} \pm |-\alpha\rangle_c |-\alpha\rangle_{c'}, \quad (29)$$

$$|\mathcal{B}_{3,4}\rangle_{cc'} \propto |\alpha\rangle_c |-\alpha\rangle_{c'} \pm |-\alpha\rangle_c |\alpha\rangle_{c'}, \quad (30)$$

respectively. In addition, the error projection operator $\hat{O}_e = |0\rangle_A \langle 0| \otimes |0\rangle_B \langle 0|$ should also be considered because there is possibility for both detectors not to register anything, even though such probability approaches zero for $\alpha \gg 1$.

In the calculation to obtain the output density matrix when the element of the parity measurement \hat{O}_1 is measured, the terms such as $|0\rangle_c |\sqrt{2}\beta\rangle_{c'}$ and $|0\rangle_c |-\sqrt{2}\beta\rangle_{c'}$ in Eq. (24) are erased from the resultant density matrix due to the orthogonality of vacuum state in these terms and nonzero number states contained in \hat{O}_1 . Other terms form the same factor $\sum_{n=1}^{\infty} (2n|\sqrt{2}\beta\rangle \langle \pm\sqrt{2}\beta|2n) = \cosh(2\beta^2) - 1$, which is factored out into the normalization factor. When \hat{O}_2 , \hat{O}_3 , and \hat{O}_4 are measured in the parity measurements, the unitary transforms required are Pauli matrices $(\sigma_z)_p$, $(\sigma_x)_p$, and $(\sigma_y)_p$ in the basis set of $\{|H\rangle, |V\rangle\}$, respectively.

The overall effect of the Bell-state measurement and unitary transform is found to be replacement of $|t\alpha\rangle_{c'}$ ($t\alpha|_{c'}$) with a (a^*) and $|-\alpha\rangle_{c'}$ ($-\alpha|_{c'}$) with b (b^*) in the teleportation channel $\rho_{pc}(t; \alpha)$ in Eq. (4). We obtain, after the normalization,

$$\rho_{out}^{c \rightarrow p} = \frac{\text{Tr}_{cc'}\{(\hat{O}_1 U_{BS})_{cc'} [\rho_{pc}(t; \alpha) \otimes |\psi_t\rangle_c \langle \psi_t|] (U_{BS}^\dagger)_{cc'}\}}{\text{Tr}\{(\hat{O}_1 U_{BS})_{cc'} [\rho_{pc}(t; \alpha) \otimes |\psi_t\rangle_c \langle \psi_t|] (U_{BS}^\dagger)_{cc'}\}} \\ = t^2 |a|^2 |H\rangle_p \langle H| + t^2 |b|^2 |V\rangle_p \langle V| + (1-t^2) |0\rangle_p \langle 0| \\ + t^2 Q(t) (ab^* |H\rangle_p \langle V| + a^* b |V\rangle_p \langle H|), \quad (31)$$

where U_{BS} represents the beam splitter operator. The fidelity is then

$$F_{c \rightarrow p}(\theta, \phi) = {}_p \langle \psi_t | \rho_{out}^{c \rightarrow p} | \psi_t \rangle_p \\ = t^2 [|a|^4 + |b|^4 + Q(t)|a|^2|b|^2], \quad (32)$$

and its average can be calculated in a similar way as for Eq. (18):

$$F_{c \rightarrow p}(t) = t^2 \left(\frac{2}{3} + \frac{Q(t)}{3} \right). \quad (33)$$

We also consider the classical limits of teleportation fidelity for comparison. Here, a classical limit means the maximum average fidelity of teleportation (disembodied transport of an unknown quantum state) by means of a classical communication channel without any entanglement. It is well known that the classical limit of fidelity for teleporting a qubit using the standard teleportation protocol is $2/3$ [37]. It can be directly applied when teleporting a coherent-state qubit to a polarization qubit ($c \rightarrow p$). However, due to the nonorthogonality of two coherent states, the classical limit for teleportation from polarization to coherent-state qubits ($p \rightarrow c$) is larger than $2/3$. A simple way to consider the classical limit is as follows: The optimal output state of teleportation without quantum entanglement is $\rho_{cl} = |a|^2 |t\alpha\rangle \langle t\alpha| + |b|^2 |-\alpha\rangle \langle -\alpha|$, where the

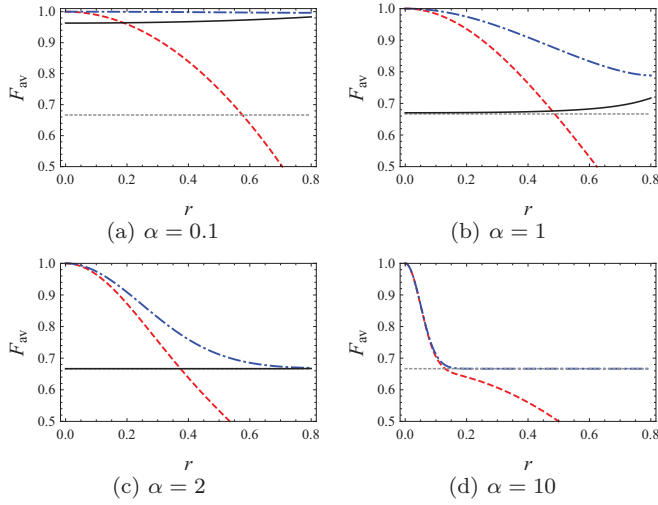


FIG. 2. (Color online) Average fidelities of teleportation from polarization to coherent-state qubits ($p \rightarrow c$, dot-dashed curves) and of teleportation in the opposite direction ($c \rightarrow p$, dashed curves) for several values of α . The classical limits $F_{cl}^{p \rightarrow c}$ (solid lines) for $p \rightarrow c$ and $2/3$ (dotted lines) for $c \rightarrow p$ are plotted for comparison.

amplitude decay was also considered. This state is obtained by preparing either state $|t\alpha\rangle \langle t\alpha|$ or state $| -t\alpha\rangle \langle -t\alpha|$ depending on the measurement outcomes of the input state. The average fidelity with the target state $|\psi_t\rangle_c$ is

$$F_{cl}^{p \rightarrow c}(t) = \langle \langle \psi_t | \rho_{cl} | \psi_t \rangle \rangle_{\theta, \phi} = \frac{S + 3S^3 - (S^4 - 1)}{4S^3} \sinh^{-1} \left[\frac{S}{\sqrt{1 - S^2}} \right]. \quad (34)$$

In the limit of $\alpha \rightarrow \infty$ where the two-basis coherent states become orthogonal, $F_{cl}^{p \rightarrow c}(t)$ approaches $2/3$.

In Fig. 2, we plot the time evolution of average teleportation fidelities for different coherent-state amplitudes $\alpha = 0.1, 1, 2, 10$ against the normalized time r . When α is large, the teleportation fidelities of both directions $p \leftrightarrow c$ decrease rapidly down to the classical limit after short time as shown in Fig. 2(d). This result is in agreement with the fast decay of entanglement in the channel presented in Fig. 1. When α is relatively small, the average fidelity for the teleportation $p \leftrightarrow c$ is close to 1 in spite of the small amount of entanglement in the channel shown in Fig. 1. This can be attributed to the effect of nonorthogonality between coherent states $|t\alpha\rangle$ and $| -t\alpha\rangle$.

In our analysis, as implied in Fig. 2, the fidelity of teleportation from polarization to coherent-state qubit ($p \rightarrow c$) is shown to be always larger than that of teleportation in the opposite direction ($c \rightarrow p$). In the region over the classical limit $2/3$, the gap between these two fidelities for a given r decreases as α becomes larger as shown in Fig. 2. This gap can be obtained and explained as follows: In the limit of large α , the output state of the teleportation ($p \rightarrow c$) in Eq. (16) can be approximated as

$$\rho_{out}^{p \rightarrow c} \approx |a|^2 |t\alpha\rangle_c \langle t\alpha| + |b|^2 | -t\alpha\rangle_c \langle -t\alpha| + Q(t)(ab^* |t\alpha\rangle_c \langle -t\alpha| + a^*b | -t\alpha\rangle_c \langle t\alpha|). \quad (35)$$

The comparison between the output state for $p \rightarrow c$ in Eq. (35) and the output state for $c \rightarrow p$ in Eq. (31) implies that the difference between $F_{c \rightarrow p}$ and $F_{p \rightarrow c}$ for large values of α can be

attributed to the term $(1 - t^2) |0\rangle_p \langle 0|$ in Eq. (31). The fidelity between the output state in Eq. (35) and the target state $|\psi_t\rangle_c$ is $|a|^4 + |b|^4 + 2Q(t)|a||b|$ and its average is calculated to be $[2 + Q(t)]/3$. By subtracting Eq. (33) from this, we obtain the gap between the two fidelities as $(1 - t^2)[2 + Q(t)]/3$. In the limit of $\alpha \rightarrow \infty$, the gap at time t_{cl} that satisfies $F_{c \rightarrow p}(t_{cl}) = 2/3$ approaches zero.

In further detail, the difference between $F_{p \rightarrow c}$ and $F_{c \rightarrow p}$ can be explained by two effects: (i) the overlap between $|t\alpha\rangle$ and $| -t\alpha\rangle$ which is dominant at the region $t\alpha \ll 1$, and (ii) the effect that the polarization qubit turns into the vacuum state by photon loss so that the output can no longer be in the original qubit space: this is not the case for the dynamic qubit basis using $|\pm t\alpha\rangle$. In the case of $p \rightarrow c$, the vacuum introduced by photon loss is detected during the Bell-state measurement and discarded by virtue of its particlelike nature. This filtering effect in the Bell-state measurement for the polarization qubits enhances the fidelity $F_{p \rightarrow c}$ over $F_{c \rightarrow p}$. While the average fidelity $F_{p \rightarrow c}$ is always higher than the classical limit, $F_{c \rightarrow p}$ degrades below its classical limit because of the vacuum component in the output state.

B. Success probabilities

An event of the teleportation process should be discarded either when the Bell-state measurement fails or when the appropriate unitary transform is unavailable. Due to these discarded events, the success probability of the teleportation process becomes less than unity. We first consider the teleportation of $p \rightarrow c$. The Bell-state measurement for the teleportation of $p \rightarrow c$ is to distinguish the four Bell states of polarization qubits. This type of Bell-state measurement can identify only two of the four Bell states [36]. As briefly explained in the previous subsection, the choice of two successful outcomes can be made arbitrary with a few simple gate operations. We here take $|B_1\rangle_{pp'}$ and $|B_3\rangle_{pp'}$ as successful outcomes and discard the other results. Considering these inherent limitations, the success probability of teleportation $p \rightarrow c$ cannot exceed $1/2$. Beside these, a failure of the Bell-state measurement also occurs when the photon is lost from the channel in the polarization qubit part. Such loss can be immediately noticed at the detectors used for the Bell-state measurement and should be considered for the success probability.

The success probability for a specific input state is

$$P(\theta, \phi) = \text{Tr}[(|B_1\rangle_{pp'} \langle B_1| + |B_3\rangle_{pp'} \langle B_3|) \{ |\psi_t\rangle_p \langle \psi_t| \otimes \rho_{p'c}(t; \alpha) \}].$$

In fact, the explicit form of $P(\theta, \phi)$ is obtained during the normalization of the output state $\rho_{out}^{p \rightarrow c}$ as the inverse of the normalization factor as implied in Eqs. (12) and (16). We find $P_{p \rightarrow c}(\theta, \phi) = t^2(1 + A \sin \theta \cos \phi)/2$ and the total success probability over all of the input states can be calculated by

$$P_{p \rightarrow c}(t) = \langle P_{p \rightarrow c}(\theta, \phi) \rangle_{\theta, \phi} = \frac{t^2}{2}. \quad (36)$$

On the other hand, teleportation for $c \rightarrow p$ can be performed with a high probability close to unity only using linear optics. This is due to the two following reasons: First, the Bell-state measurement for the coherent-state qubits, required for the

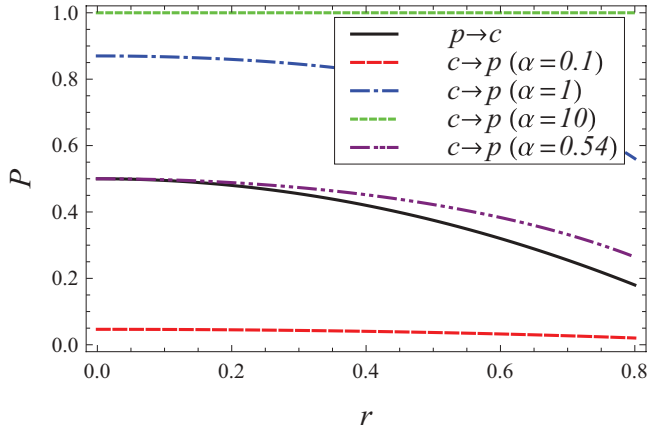


FIG. 3. (Color online) Success probability for teleportation between polarization and coherent qubits for different coherent state amplitudes ($\alpha = 0.1, 1, 0.54, 10$) against the normalized time r under decoherence.

sender's site in this process, can discriminate between all four Bell states [10]. Second, the single-qubit unitary transforms for the polarization qubit, to be performed in the receiver's site, are straightforward for any outputs. The results are discarded only when no photons are detected in the Bell-state measurement. Of course, when loss caused by decoherence occurs, the parity measurement scheme used for the Bell-state measurements in the coherent-state basis cannot filter out "wrong results" in the polarization part, which is obviously different from the Bell-state measurement with polarization qubits, and this type of error will be reflected in the degradation of the fidelity.

The success probability of $c \rightarrow p$ teleportation for a given input state is then obtained by

$$P_{c \rightarrow p}(\theta, \phi) = \sum_i \langle U_{BS}^\dagger \hat{O}_i U_{BS} \rangle = (1 - S)/(1 + S \sin \theta \cos \phi), \quad (37)$$

where the \hat{O}_i are the projection operators introduced in the previous subsection and U_{BS} is the operator for the 50:50 beam splitter. The success probability of all input states can be calculated in the same way described above, and the result is

$$P_{c \rightarrow p}(t) = \frac{S^{-1} - 1}{2} \ln \left(\frac{1 + S}{1 - S} \right). \quad (38)$$

The success probabilities in Eqs. (36) and (38) are plotted and compared for several values of α in Fig. 3. The success probability $P_{p \rightarrow c}(t)$ is invariant under the change of α , while $P_{c \rightarrow p}(t)$ becomes larger as α increases. As the hybrid channel undergoes decoherence, both $P_{p \rightarrow c}(t)$ and $P_{c \rightarrow p}(t)$ decrease due to photon losses. The decrease of $P_{c \rightarrow p}(t)$ becomes negligible for $\alpha \gg 1$ as the proportion of the vacuum state in the coherent state is very small. When $\alpha \approx 0.54$, probabilities $P_{p \rightarrow c}(t)$ and $P_{c \rightarrow p}(t)$ become comparable for all ranges of r .

V. TELEPORTATION BETWEEN POLARIZATION AND SINGLE-RAIL FOCK-STATE QUBITS

In this section, we go on to investigate teleportation between polarization and single-rail Fock-state qubits ($p \leftrightarrow s$) using the hybrid state $\rho_{ps}(t)$ in Eq. (5). Let us first consider teleportation

from a polarization qubit to a single-rail Fock-state qubit ($p \rightarrow s$). When $|B_1\rangle_{pp'}$ is detected in the Bell-state measurement for input state $|\psi_t\rangle_p = a|H\rangle_p + b|V\rangle_p$, the output state can be obtained using Eq. (12) as

$$\rho_{B_{1,2}}^{p \rightarrow s} = |a|^2 |0\rangle_s \langle 0| + |b|^2 t^2 |1\rangle_s \langle 1| + |b|^2 (1 - t^2) |0\rangle_s \langle 0| + t(ab^* |0\rangle_s \langle 1| + a^* b |1\rangle_s \langle 0|), \quad (39)$$

and no unitary transform is required. If $|B_2\rangle_{pp'}$ is measured, a single-qubit operation $(\sigma_z)_s$ is required to reconstruct $\rho_{B_{1,2}}^{p \rightarrow s}$ in Eq. (39). A phase shifter, described by $\exp(i\varphi a^\dagger a)$ with $\varphi = \pi$, can be used to perform this operation. The Bell-state measurement using linear optics cannot identify $|B_3\rangle_{pp'}$ or $|B_4\rangle_{pp'}$. Furthermore, the $(\sigma_x)_s$ operation required to implement the bit flip, $|0\rangle \leftrightarrow |1\rangle$, is difficult to realize using linear optics. We thus take only $|B_1\rangle_{pp'}$ and $|B_2\rangle_{pp'}$ as successful Bell measurement outcomes. The probability to obtain either of these outcomes is found to be

$$P_{p \rightarrow s}(\theta, \phi) = \text{Tr}[(|B_1\rangle_{pp'} \langle B_1| + |B_2\rangle_{pp'} \langle B_2|) \times \{|\psi_t\rangle_p \langle \psi_t| \otimes \rho_{p's}(t; \alpha)\}] = t^2/2 \quad (40)$$

and is independent of the input state. The fidelity of state of Eq. (39) to the target state $|\psi_t\rangle_s = a|0\rangle_s + b|1\rangle_s$ is

$$F_{p \rightarrow s}(a, b) = {}_s \langle \psi_t | \rho_{B_{1,2}}^{p \rightarrow s} | \psi_t \rangle_s = |a|^4 + |b|^4 t^2 + (1 - t^2)|a|^2 |b|^2 + 2t|a|^2 |b|^2. \quad (41)$$

The average fidelity is obtained using Eq. (18) as

$$F_{p \rightarrow s}(t) = \frac{t^2 + 2t + 3}{6}. \quad (42)$$

Let us now consider the teleportation in the opposite direction $s \rightarrow p$. The Bell measurement in the single-rail Fock-state qubit part can be performed as follows: After passing through a 50:50 beam splitter, two of the Bell states are changed as follows: $|B_3\rangle_{ss'} = 2^{-1/2}(|1\rangle_s |0\rangle_{s'} + |0\rangle_s |1\rangle_{s'}) \rightarrow |1\rangle |0\rangle$ and $|B_4\rangle_{ss'} = 2^{-1/2}(|1\rangle_s |0\rangle_{s'} - |0\rangle_s |1\rangle_{s'}) \rightarrow |0\rangle |1\rangle$. As the result, the two Bell states can simply be discriminated using two photodetectors at two output ports of the beam splitter. However, the other two Bell states cannot be distinguished using linear optics. If the outcome of the Bell-state measurement is $|B_3\rangle_{ss'}$ or $|B_4\rangle_{ss'}$, the output state after an appropriate unitary transform is

$$\rho_{B_{3,4}} = \frac{t^4 |a|^2 + t^2 (1 - t^2) |b|^2}{4P_3} |H\rangle_p \langle H| + \frac{t^2 |b|^2}{4P_3} |V\rangle_p \langle V| + \frac{t^2 (1 - t^2) |a|^2 + (1 - t^2) (2 - t^2) |b|^2}{4P_3} |0\rangle_p \langle 0| + \frac{t^3 (ab^* |H\rangle_p \langle V| + a^* b |V\rangle_p \langle H|)}{4P_3}, \quad (43)$$

with success probability $P_{3,4}(\theta, \phi) = [(2 - t^2)|b|^2 + t^2|a|^2]/4$ obtained in the same way as Eq. (40). The average success probability is found to be $P_{s \rightarrow p}(t) = \langle P_{3,4}(\theta, \phi) \rangle_{\theta, \phi} = 1/2$.

The fidelity of $\rho_{B_{3,4}}$ to the target state $|\psi_t\rangle_p = a|H\rangle_p + b|V\rangle_p$ is straightforwardly obtained as

$$F_{s \rightarrow p}(\theta, \phi) = {}_p\langle \psi_t | \rho_{B_{3,4}} | \psi_t \rangle_p = \frac{t^4 |a|^4 + t^2(1+2t-t^2)|a|^2|b|^2 + t^2|b|^4}{4P_3}, \quad (44)$$

and the average fidelity over all possible input states is

$$F_{s \rightarrow p}(t) = t^4 A_1 + t^2 A_2 + t^2(1+2t-t^2) A_3, \quad (45)$$

where

$$A_1 = \left\langle \frac{|a|^4}{4P_3} \right\rangle_\theta = \frac{c_1^2 - 4c_1c_2 + 3c_2^2 + 2c_2^2 \ln \left[\frac{c_1}{c_2} \right]}{2(c_1 - c_2)^3},$$

$$A_2 = \left\langle \frac{|b|^4}{4P_3} \right\rangle_\theta = \frac{-3c_1^2 + 4c_1c_2 - c_2^2 + 2c_1^2 \ln \left[\frac{c_1}{c_2} \right]}{2(c_1 - c_2)^3}, \quad (46)$$

$$A_3 = \left\langle \frac{|a|^2|b|^2}{4P_3} \right\rangle_\theta = \frac{c_1^2 - c_2^2 - 2c_1c_2 \ln \left[\frac{c_1}{c_2} \right]}{2(c_1 - c_2)^3},$$

with $c_1 = t^2$ and $c_2 = 2 - t^2$.

We plot the teleportation fidelities in Fig. 4(a) and the success probabilities in Fig. 4(b). We observe that the teleportation fidelity of $p \rightarrow s$ is higher than that of $s \rightarrow p$ because loss in the polarization qubit can be detected during the Bell-state measurement and discarded, while its success probability is thus lower, as shown in Fig. 4(b). The teleportation $s \rightarrow p$ succeeds with probability 1/2 regardless of r because any

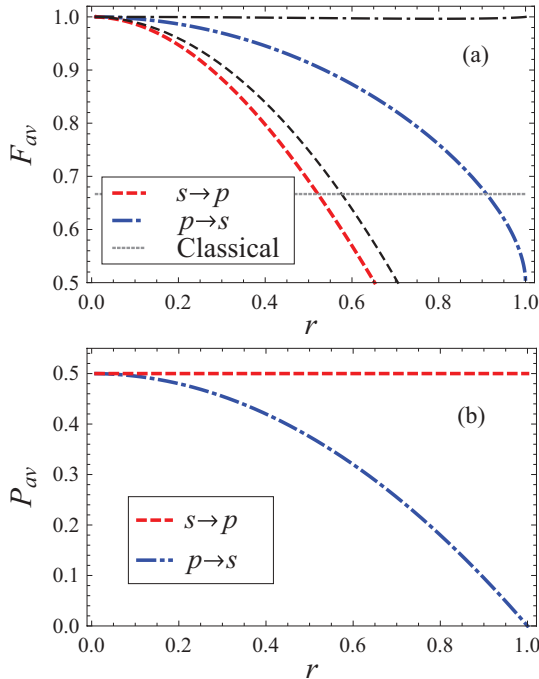


FIG. 4. (Color online) (a) Teleportation fidelities of polarization to single-rail Fock-state qubit $p \rightarrow s$ (blue dot dashed) and the opposite $s \rightarrow p$ (red dashed). Teleportation fidelities of polarization to coherent-state qubit (black dot dashed) and the opposite direction (black dashed) are drawn for comparison. (b) Success probability of teleportation of polarization to single-rail Fock-state qubit $p \rightarrow s$ (blue dot dashed) and the opposite $s \rightarrow p$ (red dashed).

decohered single-rail Fock-state qubit remains within the original qubit space and loss is not detected during the Bell-state measurement. Comparing Figs. 2 and 4, we observe that the teleportation fidelity of $p \leftrightarrow c$ with small α is higher than that of $p \leftrightarrow s$, although ρ_{ps} contains more entanglement than ρ_{pc} as shown in Fig. 1. This can also be understood as the effect of the basis overlap in coherent-state qubits.

VI. TELEPORTATION WITH POSTSELECTION ON PHOTON ARRIVAL

We attempt in this section to take into account the effect of postselection on the photon arrival at the receiver's site, while in the previous sections the teleportation fidelity and success probability were calculated considering all of the cases regardless of whether the photon arrived successfully or not (*nonpostselected* teleportation). It was clearly pointed out in Ref. [38] that considering only the postselected data to calculate the fidelity without resorting to operational means of the postselection can be misleading. In the context of our work, it should be noted that the input qubit to be teleported is an unknown one and should remain unknown after the teleportation for successive use in QIP. There exists a linear-optical method to implement quantum-nondemolition detection of single photons that leaves the polarization invariant [39] by adopting additional teleportation of the received single-polarization qubit through an ideal polarization-entangled state, which reduces the fraction of vacuum state. We shall now assume that the method in Ref. [39] is employed to implement postselection for the polarization mode.

We first observe that postselection diminishes the difference between the teleportation fidelities of the two opposite directions by filtering out the vacuum portion in the output state in the polarization mode p . Using the postselection scheme [39], the output state of teleportation from coherent to polarization qubits in Eq. (31) is converted to

$$\rho_{c \rightarrow p}^{\text{post}} = |a|^2 |H\rangle_p \langle H| + |b|^2 |V\rangle_p \langle V| + Q(t)(ab^* |H\rangle_p \langle V| + a^*b |V\rangle_p \langle H|), \quad (47)$$

thus the coherence terms decrease by the factor $Q(t) = \exp[-2\alpha^2(1-t^2)]$ due to the decoherence of the coherent-state part of the channel. The average fidelity using Eq. (18) is $F_{c \rightarrow p}^{\text{post}} = [2 + Q(t)]/3$. When $\alpha \ll 1$, $Q(t) \approx 1$ for all r and $F_{c \rightarrow p}^{\text{post}}(t) \approx 1$ as well. The comparison of Eqs. (35) and (47) shows that the two output forms become identical for $\alpha \gg 1$ in which the overlap between coherent states $|\pm \alpha\rangle$ is negligible.

In the case of $s \rightarrow p$, the postselected output state is

$$\rho_{s \rightarrow p}^{\text{post}} = \frac{t^2|a|^2 + (1-t^2)|b|^2}{4P_3} |H\rangle_p \langle H| + \frac{|b|^2}{4P_3} |V\rangle_p \langle V| + \frac{t(ab^* |H\rangle_p \langle V| + a^*b |V\rangle_p \langle H|)}{4P_3}, \quad (48)$$

and the average fidelity is changed to

$$F_{s \rightarrow p}^{\text{post}}(t) = t^2 A_1 + A_2 + (1+2t-t^2) A_3. \quad (49)$$

When this is compared with $F_{p \rightarrow s}(t)$ in Eq. (42), we find that the two fidelities are again very similar. We find that the largest difference between $F_{p \rightarrow s}(t)$ and $F_{s \rightarrow p}^{\text{post}}(t)$ is less than 0.01.

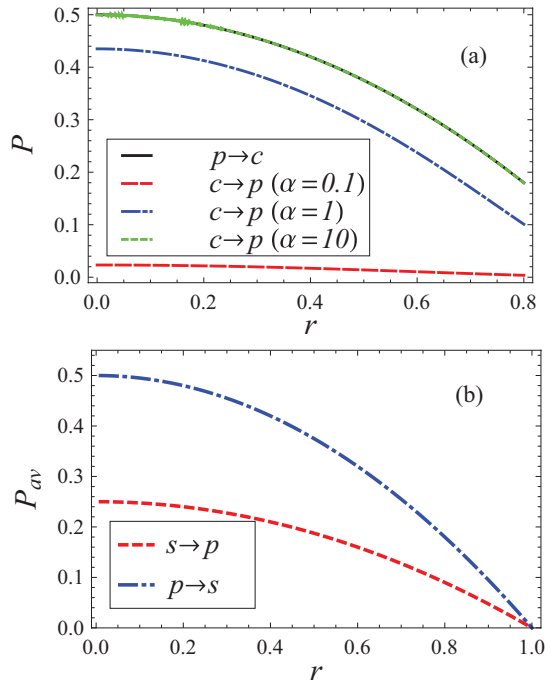


FIG. 5. (Color online) Success probabilities after postselection for output qubits in the polarization part for (a) teleportation between polarization and coherent-state qubits ($p \leftrightarrow c$) and for (b) teleportation between polarization and single-rail Fock-state qubits ($p \leftrightarrow s$). In panel (a), the curve for $P_{p \rightarrow c}$ is overlapped with the one for $P_{c \rightarrow p}$ when $\alpha = 10$. One can see that the success probabilities from the fieldlike to particlelike qubits are lower than the opposite ones, which is contrary to the cases without postselection for the output qubits in the polarization part.

It should also be noted that postselection decreases the success probability of teleportation into the polarization qubit. The postselection protocol [39] is limited by the polarization Bell measurement with its success probability $1/2$, and failures occur also due to the vacuum part [with a factor of $1 - t^2$ for states in Eqs. (31) and (43)]. A factor of $t^2/2$ should thus be multiplied in overall and the postselected probabilities $P_{c,s \rightarrow p}^{\text{post}}(t) = t^2 P_{c,s \rightarrow p}(t)/2$ are lowered below $P_{p \rightarrow c,s}(t)$, respectively. Probabilities $P_{c \rightarrow p}^{\text{post}}(t)$ and $P_{p \rightarrow c}(t)$ become identical only when $\alpha \gg 1$. We have plotted success probabilities in Fig. 5.

VII. REMARKS

We have investigated quantum teleportation between two different types of optical qubits under the effects of decoherence caused by photon losses: one type is particlelike such as photon-polarization qubit and the other is fieldlike such as coherent-state or Fock-state qubits. The teleportation fidelities and success probabilities depend on the “direction” of teleportation; namely, whether teleportation is performed

from one type of qubit to the other or from the latter to the former.

The average fidelity of teleportation from particlelike to fieldlike qubits is shown to be larger than the opposite direction under decoherence. This is due to the asymmetry of photon losses in the hybrid channel as well as to the possibility of detecting losses in Bell-state measurements. In the case of teleportation from a single-photon qubit using the polarization degree of freedom, the sender can notice photon loss during the Bell-state measurement in the polarization qubit part by virtue of its particlelike nature (i.e., definite number of particles). Since the cases with losses are discarded, this enhances the teleportation fidelity. Even with a teleportation channel containing very small entanglement, it is possible to obtain a large teleportation fidelity by filtering the failures in Bell-state measurements.

The nonorthogonality of the two coherent states that form a qubit basis is another major factor that affects the teleportation fidelity. For example, the fidelity of teleportation from polarization to coherent-state qubits with small α is always higher than that with large α due to the larger overlap of the qubit basis for smaller α . However, in order to make a fair comparison, it is important to note that this nonorthogonality for small α also increases the classical limit of quantum teleportation.

In terms of success probabilities, teleportation from fieldlike to particlelike qubits shows higher values. For example, in the case of teleportation from coherent-state to polarization qubits, the success probability increases up to 1 as the amplitude of the coherent-state qubit becomes large.

The effect of postselection has been investigated as a trial to increase the fidelity on the particlelike sides. As a result, the fidelities of the teleportation from fieldlike to particlelike qubits increase and become almost the same as those in the opposite direction. However, the additional resources (i.e., preparation of additional polarization entangled states) and the decrease of the success probabilities are the price to be paid.

Our work may provide useful information in the context of information transfer between systems of different properties. As an example, since a coherent state with a large amplitude contains a large number of photons, the hybrid channel in Eq. (1) can be considered to be entanglement between microscopic and macroscopic systems [35,40–45]. Our study may be a framework to study information transfer between microscopic and macroscopic systems.

ACKNOWLEDGMENTS

This work was supported by the National Research Foundation of Korea (NRF) grant funded by the Korean Government (No. 3348-20100018) and the World Class University program.

[1] P. Kok, W. J. Munro, K. Nemoto, T. C. Ralph, J. P. Dowling, and G. J. Milburn, *Rev. Mod. Phys.* **79**, 135 (2007).
 [2] J. L. O’Brien, *Science* **318**, 1567 (2007).

[3] T. C. Ralph and G. J. Pryde, *Prog. Opt.* **54**, 209 (2010).
 [4] E. Knill, R. Laflamme, and G. J. Milburn, *Nature (London)* **409**, 46 (2001).

- [5] A. P. Lund and T. C. Ralph, *Phys. Rev. A* **66**, 032307 (2002).
- [6] P. T. Cochrane, G. J. Milburn, and W. J. Munro, *Phys. Rev. A* **59**, 2631 (1999).
- [7] H. Jeong and M. S. Kim, *Phys. Rev. A* **65**, 042305 (2002).
- [8] T. C. Ralph, A. Gilchrist, G. J. Milburn, W. J. Munro, and S. Glancy, *Phys. Rev. A* **68**, 042319 (2003).
- [9] H. Jeong and T. C. Ralph, arXiv:quant-ph/0509137.
- [10] H. Jeong, M. S. Kim, and J. Lee, *Phys. Rev. A* **64**, 052308 (2001).
- [11] H. Jeong and M. S. Kim, *Quantum Inf. Comput.* **2**, 208 (2002).
- [12] S. J. van Enk and O. Hirota, *Phys. Rev. A* **64**, 022313 (2001).
- [13] A. P. Lund, T. C. Ralph, and H. L. Haselgrove, *Phys. Rev. Lett.* **100**, 030503 (2008).
- [14] K. Park and H. Jeong, *Phys. Rev. A* **82**, 062325 (2010).
- [15] K. Nemoto and W. J. Munro, *Phys. Rev. Lett.* **93**, 250502 (2004).
- [16] W. J. Munro, Kae Nemoto, and T. P. Spiller, *New J. Phys.* **7**, 137 (2005).
- [17] H. Jeong, *Phys. Rev. A* **72**, 034305 (2005).
- [18] H. Jeong, *Phys. Rev. A* **73**, 052320 (2006).
- [19] P. van Loock, W. J. Munro, Kae Nemoto, T. P. Spiller, T. D. Ladd, Samuel L. Braunstein, and G. J. Milburn, *Phys. Rev. A* **78**, 022303 (2008).
- [20] P. van Loock, *Laser Photonics Rev.* **5**, 167 (2011).
- [21] S.-W. Lee and H. Jeong, arXiv:1112.0825.
- [22] C. H. Bennett, G. Brassard, C. Crépeau, R. Jozsa, A. Peres, and W. K. Wootters, *Phys. Rev. Lett.* **70**, 1895 (1993).
- [23] D. Bouwmeester, J.-W. Pan, K. Mattle, M. Eibl, H. Weinfurter, and A. Zeilinger, *Nature (London)* **390**, 575 (1997).
- [24] T. C. Ralph, A. P. Lund, and H. M. Wiseman, *J. Opt. B: Quantum Semiclassical Opt.* **7**, S245 (2005).
- [25] C. C. Gerry, *Phys. Rev. A* **59**, 4095 (1999).
- [26] J. H. Shapiro, *Phys. Rev. A* **73**, 062305 (2006).
- [27] J. H. Shapiro and M. Razavi, *New J. Phys.* **9**, 16 (2007).
- [28] J. Gea-Banacloche, *Phys. Rev. A* **81**, 043823 (2010).
- [29] S. J. D. Phoenix, *Phys. Rev. A* **41**, 5132 (1990).
- [30] K. Życzkowski, P. Horodecki, A. Sanpera, and M. Lewenstein, *Phys. Rev. A* **58**, 883 (1998); A. Peres, *Phys. Rev. Lett.* **77**, 1413 (1996); M. Horodecki, P. Horodecki, and R. Horodecki, *Phys. Lett. A* **223**, 1 (1996); J. Lee, M. S. Kim, Y.-J. Park, and S. Lee, *J. Mod. Opt.* **47**, 2151 (2000).
- [31] G. Vidal and R. F. Werner, *Phys. Rev. A* **65**, 032314 (2002).
- [32] M. S. Kim and V. Bužek, *Phys. Rev. A* **46**, 4239 (1992).
- [33] D. Wilson, H. Jeong, and M. S. Kim, *J. Mod. Opt.* **49**, 851 (2002).
- [34] H. Jeong, J. Lee, and M. S. Kim, *Phys. Rev. A* **61**, 052101 (2000).
- [35] J. Park, M. Saunders, Y.-I. Shin, K. An, and H. Jeong, *Phys. Rev. A* **85**, 022120 (2012).
- [36] N. Lütkenhaus, J. Calsamiglia, and K.-A. Suominen, *Phys. Rev. A* **59**, 3295 (1999).
- [37] S. Massar and S. Popescu, *Phys. Rev. Lett.* **74**, 1259 (1995).
- [38] P. Kok and S. L. Braunstein, *Phys. Rev. A* **61**, 042304 (2000).
- [39] P. Kok, H. Lee, and J. P. Dowling, *Phys. Rev. A* **66**, 063814 (2002).
- [40] K. Wódkiewicz, *New J. Phys.* **2**, 21 (2000).
- [41] H. Jeong and T. C. Ralph, *Phys. Rev. Lett.* **97**, 100401 (2006).
- [42] H. Jeong and T. C. Ralph, *Phys. Rev. A* **76**, 042103 (2007).
- [43] F. De Martini, F. Sciarrino, and C. Vitelli, *Phys. Rev. Lett.* **100**, 253601 (2008).
- [44] N. Spagnolo, C. Vitelli, F. Sciarrino, and F. De Martini, *Phys. Rev. A* **82**, 052101 (2010).
- [45] N. Spagnolo, C. Vitelli, M. Paternostro, F. De Martini, and F. Sciarrino, *Phys. Rev. A* **84**, 032102 (2011).